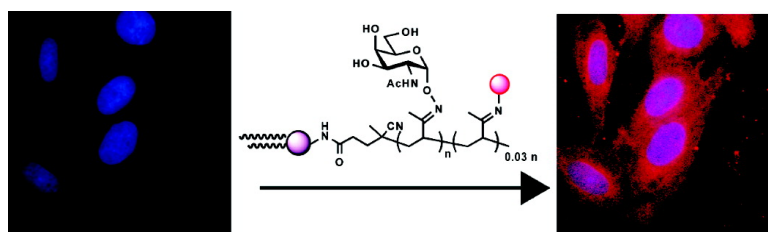Article

Noncovalent Cell Surface Engineering: Incorporation of Bioactive Synthetic Glycopolymers into Cellular Membranes

David Rabuka, Martin B. Forstner, Jay T. Groves, and Carolyn R. Bertozzi

More About This Article

Additional resources and features associated with this article are available within the HTML version:

- Supporting Information
- Links to the 1 articles that cite this article, as of the time of this article download
- Access to high resolution figures
- Links to articles and content related to this article
- Copyright permission to reproduce figures and/or text from this article

View the Full Text HTML

Noncovalent Cell Surface Engineering: Incorporation of Bioactive Synthetic Glycopolymers into Cellular Membranes

David Rabuka,[†] Martin B. Forstner,[†] Jay T. Groves,[†,||] and
Carolyn R. Bertozzi*,[†,‡,§,||,⊥]

*Departments of Chemistry, Molecular and Cell Biology, Howard Hughes Medical Institute,
University of California, Materials Sciences Division, The Molecular Foundry, Lawrence
Berkeley National Laboratory, Berkeley, California 94720*

Received November 27, 2007; E-mail: crb@berkeley.edu

Abstract: The controlled addition of structurally defined components to live cell membranes can facilitate the molecular level analysis of cell surface phenomena. Here we demonstrate that cell surfaces can be engineered to display synthetic bioactive polymers at defined densities by exogenous membrane insertion. The polymers were designed to mimic native cell-surface mucin glycoproteins, which are defined by their dense glycosylation patterns and rod-like structures. End-functionalization with a hydrophobic anchor permitted incorporation into the membranes of live cultured cells. We probed the dynamic behavior of cell-bound glycopolymers bearing various hydrophobic anchors and glycan structures using fluorescence correlation spectroscopy (FCS). Their diffusion properties mirrored those of many natural membrane-associated biomolecules. Furthermore, the membrane-bound glycopolymers were internalized into early endosomes similarly to endogenous membrane components and were capable of specific interactions with protein receptors. This system provides a platform to study cell-surface phenomena with a degree of chemical control that cannot be achieved using conventional biological tools.

Introduction

Many biological activities of cell-surface glycans can only be studied in the context of living cells. In addition to a glycan's primary structure, the architecture of its protein scaffold as well as its density and distribution on the cell surface can all contribute to biological activity.[1] Furthermore, many glycans participate in complex cellular signaling pathways that can only be probed using live cells. Unfortunately, the heterogeneous nature of cell surfaces, particularly with respect to glycoconjugate structures, has frustrated molecular-level studies of glycan function. Considerable effort has been directed to modeling cell surfaces in wholly synthetic membrane systems built from the bottom up.[2–5] These model membranes benefit from well-defined chemical composition but lack the dynamics and biological response capabilities of live cells. Thus, an appealing complement to model membrane studies is to engineer well-defined glycoconjugates within the context of live cell membranes.

Several approaches to cell surface engineering have been reported.[6] Straightforward genetic techniques can be employed to express heterologous proteins on cells but are less useful for manipulation of cell-surface glycans or lipids. By contrast, all three biomolecule classes can be manipulated within the cell surface context using chemical approaches. For example, metabolic labeling of cell surface biomolecules with a bioorthogonal chemical reporter allows for subsequent covalent attachment of tailored synthetic epitopes.[7–10] A drawback of both genetic and metabolic engineering approaches is their reliance upon the cell's internal machinery. Both methods inevitably perturb the cell's physiology, possibly obscuring the biological response under investigation. Moreover, some cell types are simply refractory to exogenous gene expression or metabolic tampering.

For these reasons, passive exogenous insertion of chemically defined structures into cellular membranes is an attractive alternative approach to cell surface engineering.[11] The approach entails conjugating the epitope of interest to a suitable hydrophobic anchor, such as a fatty acid,[12,13] steroid,[14] lipophilic

[†] Departments of Chemistry, University of California.
[‡] Molecular and Cell Biology, University of California.
[§] Howard Hughes Medical Institute, University of California.
[||] Materials Sciences Division, Lawrence Berkeley National Laboratory.
[⊥] The Molecular Foundry, Lawrence Berkeley National Laboratory.

(1) Raman, R.; Raguram, S.; Venkataraman, G.; Paulson, J. C.; Sasisekharan, R. *Nat. Meth.* **2005**, *2*, 817–824.
(2) Grogan, M. J.; Kaizuka, Y.; Conrad, R. M.; Groves, J. T.; Bertozzi, C. R. *J. Am. Chem. Soc.* **2005**, *127*, 14383–14837.
(3) Mossman, K. D.; Campi, G.; Groves, J. T.; Dustin, M. L. *Science* **2005**, *310*, 1191–1193.
(4) Paulick, M. G.; Wise, A. R.; Forstner, M. B.; Groves, J. T.; Bertozzi, C. R. *J. Am. Chem. Soc.* **2007**, *129*, 11543–11550.
(5) Rabuka, D.; Parthasarathy, R.; Lee, G. S.; Chen, X.; Groves, J. T.; Bertozzi, C. R. *J. Am. Chem. Soc.* **2007**, *129*, 5462–54671.

(6) Mahal, L. K.; Bertozzi, C. R. *Chem. Biol.* **1997**, *4*, 415–422.
(7) Sadamoto, R.; Niikura, K.; Sears, P. S.; Liu, H.; Wong, C. H.; Suksomcheep, A.; Tomita, F.; Monde, K.; Nishimura, S. *J. Am. Chem. Soc.* **2002**, *124*, 9018–9019.
(8) Link, A. J.; Tirrell, D. A. *J. Am. Chem. Soc.* **2003**, *125*, 11164–11165.
(9) Prescher, J. A.; Bertozzi, C. R. *Nat. Chem. Biol.* **2005**, *1*, 13–21.
(10) Campbell, C. T.; Sampathkumar, S. G.; Yarema, K. J. *Mol. Biosyst.* **2007**, *3*, 187–194.
(11) Peterson, B. R. *Org. Biomol. Chem.* **2005**, *3*, 3607–3612.
(12) Cox, D. L.; Radolf, J. D. *Microbiology* **2001**, *147*, 1161–1169.
(13) Amatore, C.; Arbault, S.; Bouret, Y.; Guille, M.; Lemaitre, F.; Verchier, Y. *ChemBioChem* **2006**, *7*, 1998–2003.
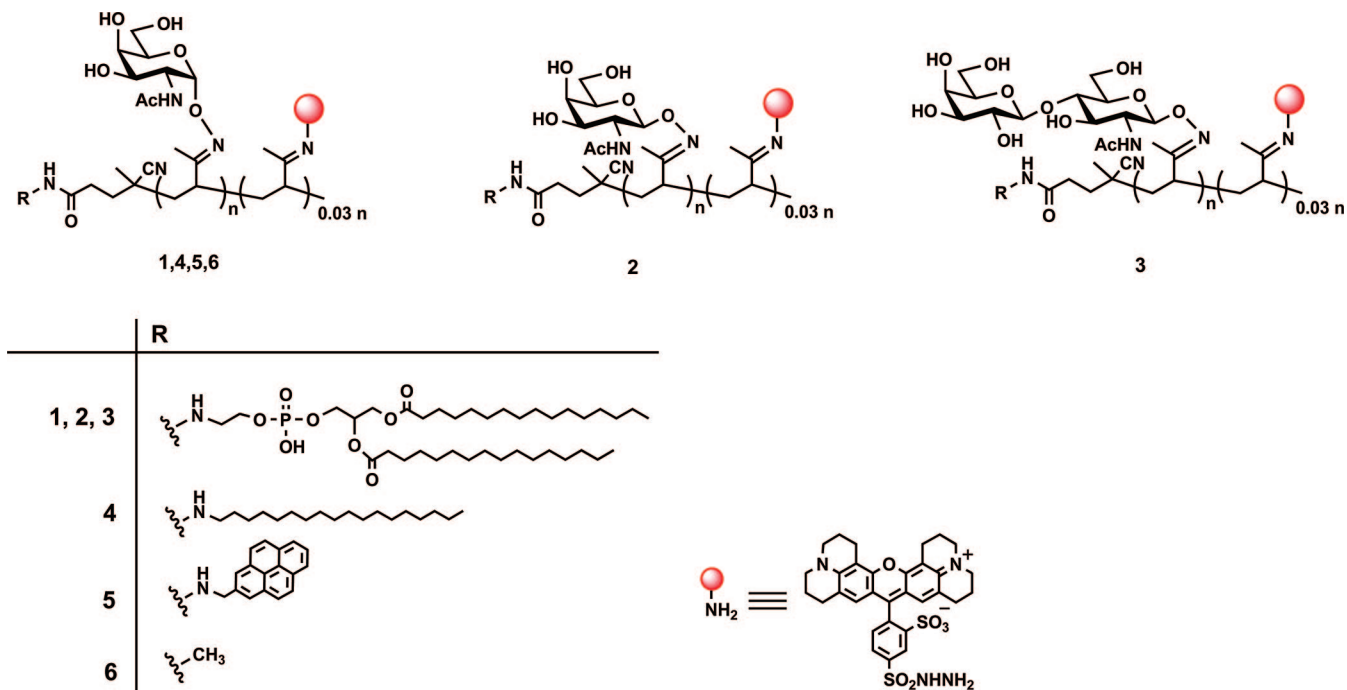
Figure 1. Chemical structures of mucin mimic glycopolymers with various glycans appended to the polymer backbone and various end groups.

peptide,[15–17] or pyrene moiety,[18] and incubating the synthetic construct with cultured cells. Glycolipids,[19] glycosylphosphatidylinositol (GPI)-anchored proteins and their analogues,[4,20] and lipid-based imaging dyes have all been displayed on cell membranes in this fashion. In some recent examples, a biological response was modulated by the newly displayed cell-surface epitope. For example, Peterson and co-workers introduced artificial Fc receptors onto cells that were capable of capturing and internalizing antibody molecules.[21,22] Henry and co-workers reprogrammed the serological properties of human red blood cells by exogenous addition of synthetic glycolipids.[23] Finally, Dowhan and co-workers altered the phenotype of a lipid-deficient *E. coli* mutant by addition of a foreign glycolipid derived from another organism to its outer membrane.[24] Inspired by these precedents, we employed noncovalent cell surface engineering as a means to display chemically defined glyco-conjugates on live cells.

In this work, we focused on synthetic glycopolymers that mimic cell surface mucins, a class of glycoproteins with roles in modulating cell−cell interactions.[25] Mucins are characterized by extended regions of densely clustered serine (Ser) and/or threonine (Thr) residues bearing O-linked glycans that initiate with α-linked N-acetylgalactosamine (GalNAc).[25,26] The closely packed glycans force the polypeptide backbone into an extended structure that is thought to project above other cell surface molecules. Altered mucin glycosylation or expression has been associated with numerous disease states. For example, endothelial mucins at sites of chronic inflammation undergo changes in glycosylation that enhance their interactions with circulating leukocytes.[27] Mucins are upregulated on some cancers and their glycans are truncated on others, transformations that have been correlated metastatic potential.[28] The molecular bases of these mucin-dependent biological events are not well understood. The ability to control a mucin's glycan structure and cell surface density would benefit studies of their biological functions.

Recently, we reported the synthesis of glycopolymers that mimic the unique structural features of mucins.[5] As shown in Figure 1, the mucin mimics comprise a poly(methyl vinyl ketone) (poly(MVK)) backbone to which synthetic glycans are appended via oxime linkages. By virtue of their densely packed glycans, the glycopolymers possess extended rod-like structures and hydrodynamic properties similar to those of native mucins. Further, the mucin mimics were end-functionalized with various hydrophobic groups, including single chain lipids, pyrene, and phospholipids. This enabled their insertion into supported lipid bilayers for biophysical studies.

(14) Kuhn-Velten, W. N.; Kempfle, M. A. *Biochim. Biophys. Acta* **1993**, *1145*, 185–190.

(15) Ceppi, P.; Colombo, S.; Francolini, M.; Raimondo, F.; Borgese, N.; Masserini, M. *Proc. Natl. Acad. Sci. U.S.A.* **2005**, *102*, 16269–16274.

(16) Ege, C.; Lee, K. Y. *Biophys. J.* **2004**, *87*, 1732–1740.

(17) Pande, A. H.; Qin, S.; Tatulian, S. A. *Biophys. J.* **2005**, *88*, 4084–4094.

(18) Brunette, D. M.; Katz, M. *Chem. Biol. Interact.* **1975**, *11*, 1–14.

(19) Schwarzmann, G. *Semin. Cell. Dev. Biol.* **2001**, *12*, 163–171.

(20) Premkumar, D. R.; Fukuoka, Y.; Sevlever, D.; Brunschwig, E.; Rosenberry, T. L.; Tykocinski, M. L.; Medof, M. E. *J. Cell Biochem.* **2001**, *82*, 234–245.

(21) Boonyarattanakalin, S.; Athavankar, S.; Sun, Q.; Peterson, B. R. *J. Am. Chem. Soc.* **2006**, *128*, 386–387.

(22) Boonyarattanakalin, S.; Martin, S. E.; Sun, Q.; Peterson, B. R. *J. Am. Chem. Soc.* **2006**, *128*, 11463–11470.

(23) Frame, T.; Carroll, T.; Korchagina, E.; Bovin, N.; Henry, S. *Transfusion* **2007**, *47*, 876–882.

(24) Wikstrom, M.; Xie, J.; Bogdanov, M.; Mileykovskaya, E.; Heacock, P.; Wieslander, A.; Dowhan, W. *J. Biol. Chem.* **2004**, *279*, 10484–10493.

(25) Hang, H. C.; Bertozzi, C. R. *Bioorg. Med. Chem.* **2005**, *13*, 5021–5034.

(26) Shogren, R.; Gerken, T. a.; Jentoft, N. *Biochemistry* **1989**, *28*, 5525–5536.

(27) Yeh, J. C.; Hiraoka, N.; Petryniak, B.; Nakayama, J.; Ellies, L. G.; Rabuka, D.; Hindsgaul, O.; Marth, J. D.; Lowe, J. B.; Fukuda, M. *Cell* **2001**, *105*, 957–969.

(28) Hollingsworth, M. A.; Swanson, B. J. *Nat. Rev. Cancer* **2004**, *4*, 45–60.

Having demonstrated that the synthetic glycopolymers act similarly to native mucins *in vitro*, we now sought to investigate their behavior on live cells. For initial studies, we chose a cell type that is devoid of endogenous mucins. The *ldlD* Chinese hamster ovary (CHO) cell line is deficient in UDP-Glc/GlcNAc C_4-epimerase. Consequently, these cells lack UDP-GalNAc, the substrate used by the polypeptide *N*-acetylgalactosaminyltransferases (ppGalNAcTs) that initiate mucin-type O-linked glycosylation.[29] We envisioned using our synthetic mucin mimics to complement these cells with respect to mucin expression. In this study we synthesized a panel of mucin mimics, demonstrated their insertion into *ldlD* CHO cell membranes, and quantified their density and mobility as a function of their glycan and hydrophobic tail structures. Finally, we demonstrated that the cell-bound mucin mimics interact with proteins in a glycan-specific manner and traffic within the cell similarly to native cell surface molecules.

Results and Discussion

Modular Synthesis of End-Functionalized Mucin-Mimic Polymers. The glycopolymers used in this study are similar to those previously reported and were synthesized by a similar route.[5] Briefly, we generated modified AIBN derivatives for use as radical initiators by coupling various lipophilic groups to 4,4′-azobis(4-cyanovaleric acid) (ACVA). In this fashion, we generated poly(MVK) functionalized with 1,2-dipalmitoyl-glycero-3-phosphoethanolamino, octadecyl, or pyrene end groups. The poly(MVK) backbones were further elaborated with α-aminooxy GalNAc,[30] β-aminooxy GalNAc or β-aminooxy *N*-acetyllactosamine (LacNAc).[5] A small fraction of the ketone groups was simultaneously reacted with Texas Red hydrazide (0.03 equiv) to afford a fluorescent probe for biophysical studies. The complete panel of glycopolymers evaluated in this study is shown in Figure 1 (**1–5**). We also prepared a glycopolymer lacking a hydrophobic tail as a control compound (α-aminooxy GalNAc-conjugated poly(MVK) with Texas Red hydrazide (0.03 equiv), compound **6**, Figure 1).

Insertion of Mucin-Mimic Polymers into *ldlD* CHO Cell Membranes and Analysis by FCS. *ldlD* CHO cells were incubated with polymers **1** and **6** for 1 h at room temperature, then washed, and imaged by fluorescence microscopy (see Experimental Methods for details). Cells treated with **1** showed robust cell surface fluorescence (Figure 2), whereas cells treated with **6** showed only low levels of background fluorescence. Under these conditions, some polymers were internalized into endocytic vesicles during the incubation period. We attempted to halt membrane internalization by cooling the cells to 4 °C, but the accompanying membrane rigidification complicated mobility studies (not shown). Higher incubation temperatures (i.e., 37 °C) led to faster internalization rates, as expected.

We employed fluorescent correlation spectroscopy (FCS) to determine the density of cell surface mucin mimics resulting from incubation with various concentrations of polymers **1** and **6** in the media. FCS is solely sensitive to moving fluorescent objects; only fluorophores (in this case, the Texas Red-labeled glycopolymers) that diffuse within the membrane or solution are detected.[31–35] The representative correlation curves shown
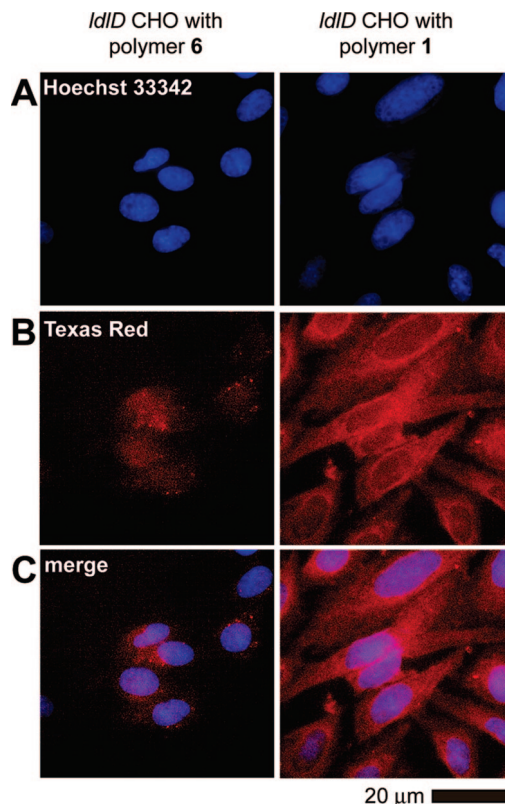

IdlD CHO with polymer **6**   *IdlD* CHO with polymer **1**

A Hoechst 33342

B Texas Red

C merge

20 μm

Figure 2. Fluorescence microscopy images of live *ldlD* CHO cells incubated for 1 h with glycopolymer **1** containing a phospholipid end group or glycopolymer **6** containing no end functionalization. The cells were stained with Hoechst 33342, a nuclear counterstain, before imaging. (A) Cells stained with Hoechst 33342 (Blue = DAPI channel). (B) Cells with Texas Red functionalized polymers **1** or **6** (Red = Texas Red channel). (C) Overlay of DAPI and Texas Red channels.

in Figure 3 illustrate that FCS readily resolved differences in mobilities and number densities between different polymers. From the measured correlations, both the mobilities of the diffusing molecules and the average number of molecules with a particular diffusive speed can be determined.

Using this technique, we measured the amount of polymers **1** and **6** incorporated into cell membranes when incubated at solution concentrations from 25 μg/mL to 1000 μg/mL (Figure 4A). The number density of membrane-associated polymer **1** increased in a dose-dependent manner from 25 μg/mL to 250 μg/mL, above which little change was observed. The observed plateau may reflect an equilibrium state in which the rate of polymer insertion into the membrane matches the rate of internalization via endocytosis. It is important to note that while there was a significant change in the number densities with increasing concentration of **1**, the mobility of the glycopolymer was unaffected. The diffusion coefficients were the same within the error margin (0.33 ± 0.06 μm²/s) regardless of the amount of polymer incorporated into the membrane (Table 1).

Polymer **6**, lacking a hydrophobic tail, showed no significant incorporation into the *ldlD* CHO cell membrane, consistent with Figure 2. The measured number densities (Figure 4A, dashed line) were substantially lower than those measured for **1**, and

(29) Jacobs, C. L.; Yarema, K. J.; Mahal, L. K.; Nauman, D. A.; Charters, N. W.; Bertozzi, C. R. *Methods Enzymol.* **2000**, *327*, 260–275.
(30) Marcaurelle, L. A.; Shin, Y. S.; Goon, S.; Bertozzi, C. R. *Org. Lett.* **2001**, *3*, 3691–3694.
(31) Schwille, P.; Korlach, J.; Webb, W. W. *Cytometry* **1999**, *36*, 176–182.

(32) Hess, S. T.; Huang, S. H.; Heikal, A. A.; Webb, W. W. *Biochemistry* **2002**, *41*, 697–705.
(33) Medina, M. A.; Schwille, P. *Bioessays* **2002**, *24*, 758–764.
(34) Sengupta, P.; Balaji, J.; Maiti, S. *Methods* **2002**, *27*, 374–387.
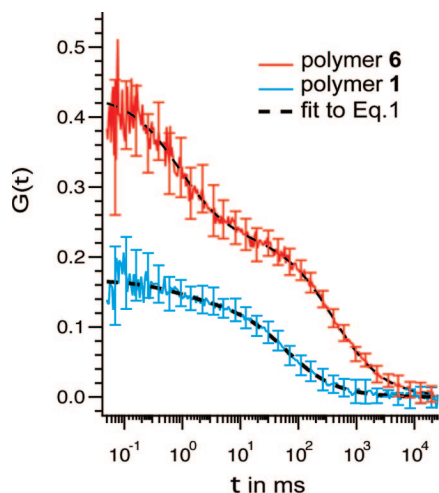(35) Haustein, E.; Schwille, P. *Methods* **2003**, *29*, 153–166.

Figure 3. Representative average cross-correlation curves from one cell for polymer **1** (blue curve) and **6** (red curve) with the standard deviation calculated from 10 individual measurements shown as error bars at every 10th data point. Clearly visible is the decay at short time scales due to residual free polymer in solution. The diffusion coefficients of the free (D_B = 26 ± 3 μm^2/s) and membrane-associated polymers and their respective number densities were determined by fitting the experimental curves to the theoretical function (eq 1) describing free diffusion of two components (dashed black lines). $G(\tau)$ = the temporal cross-correlation.

the associated diffusion coefficient, while constant throughout the investigated concentration range, was also much lower (0.05 ± 0.03 μm^2/s) than that for **1**. This suggests that the small amount of polymer **6** associated with the cells does not reside within the fluid plasma membrane; rather, the polymers may be nonspecifically bound to other cell surface components. These results demonstrate that a hydrophobic end-functional group is required for incorporation of the mucin mimic polymers into the plasma membrane.

Effect of Mucin Mimic Glycan Structures on Membrane Insertion and Mobility. We next asked whether the specific structures of the glycans attached to the polymer backbone affect its incorporation efficiency and lateral mobility on the membrane. To this end, we treated *ldlD* CHO cells with glycopolymers bearing α-GalNAc (**1**), β-GalNAc (**2**), or LacNAc (**3**) at 100 μg/mL and compared the respective number densities using FCS. As shown in Figure 4B, no significant differences in the surface densities were observed. Thus, incorporation of the polymers into the plasma membrane does not appear to depend on the precise structure of the attached glycans. The diffusion coefficients were also unaffected by changes in the glycan structure (Table 1).

Effect of Hydrophobic End-Functionality on Membrane Insertion and Mobility. We also tested a panel of hydrophobic end-functional groups with respect to membrane insertion efficiency and lateral mobility. These included a phospholipid tail similar to biological membrane lipids (**1**), a straight chain alkyl tail (**4**), and a pyrene group (**5**) (Figure 1). The cells were incubated with each polymer at 100 μg/mL for 1 h at room temperature and then subjected to FCS measurements as before (Figure 4C). Glycopolymer **1** showed the highest incorporation efficiency, followed by pyrene-terminated glycopolymer **4** and octadecyl-terminated glycopolymer **5**, respectively. By contrast, the diffusion coefficients of the three end-functionalized polymers were similar (Table 1). As before, control polymer **6** showed only background cell membrane association and low mobility. All subsequent studies were performed with glyco-

polymers bearing the phospholipid end-modification due to their superior insertion efficiency.

Comparison of the Mobility and Density of 1 with Native GPI-Anchored Proteins. We were interested in comparing the mobility and cell surface density of the membrane-associated polymers with those of native proteins. Glycosylphosphatidyl-inositol (GPI)-anchored proteins associate with the outer leaflet of the plasma membrane via lipid insertion, similar to our synthetic polymers, and thus provided a useful point of comparison. We expressed two GPI-anchored proteins, decay-accelerating factor (DAF) and folate receptor (FR), both as N-terminal green fluorescent protein (GFP) fusions, in CHO cells.[36] The cell-surface proteins were subjected to FCS analysis. DAF had a measured mobility of 0.34 ± 0.06 μm^2/s while FR had a measured mobility of 0.40 ± 0.05 μm^2/s. The phospho-lipid-functionalized polymers **1**–**3** exhibited similar mobilities (Table 1). Overall, the polymers might have slightly slower mobilities than the GPI-anchored proteins, perhaps reflecting the impeding interactions of the polymer chains with cell surface components. The two GPI-anchored proteins displayed disparate average number densities—600 ± 500 and 400 ± 200 proteins/μm^2 for GPI-DAF/GFP and GPI-FR/GFP, respectively—reflecting different expression levels in the transiently transfected CHO cells. By contrast, the highest achievable density of glycopolymer **1** was 150 ± 25 (Figure 4A). The surface density of an exogenously inserted polymer was much more consistent from cell to cell compared to endogenously expressed GPI-anchored proteins.

Interaction of Membrane-Associated Mucin Mimics with Proteins. A major function of cell-surface mucins is to guide interactions among cells via specific molecular recognition by glycan-binding proteins. We therefore assessed the ability of mucin mimics **1** (modified with α-GalNAc) and **2** (modified with β-GalNAc) to bind proteins while presented on the surface of live cell surfaces. We employed the carbohydrate-binding protein (i.e., lectin) *Helix pomatia* agglutinin (HPA), which binds α-linked GalNAc residues but not their β-linked isomers.[37]

ldlD CHO cells were incubated with Texas Red-labeled mucin mimic **1** or **2** followed by FITC labeled HPA and analyzed by flow cytometry. As shown in Figure 5A, HPA specifically bound to cells displaying α-GalNAc-polymer **1** on their surface but not to cells displaying β-GalNAc-polymer **2**. Similar results were obtained by fluorescence microscopy analysis (Figure 5B). As described above, the FCS measurements determined that polymers **1** and **2** have very similar densities on the cell membrane. Thus, the differential binding of HPA to cells displaying **1** and **2** solely reflects the intrinsic specificity of the protein for the α-linked GalNAc polymer.

Intracellular Trafficking of Mucin Mimics in *ldlD* CHO Cells. As most cell surface proteins are internalized and degraded or recycled over time, we hypothesized that the synthetic glycopolymers might also be subjected to these processes. Microscopy images revealed a rise in internalized polymer over time as judged by the appearance of intracellular Texas Red fluorescent punctae. In order to identify the path of internalization, we performed colocalization experiments using polymer **1** and Alexa Fluor 647 conjugated dextran (Dex-647), which is

(36) Paulick, M. G.; Forstner, M. B.; Groves, J. T.; Bertozzi, C. R. *Proc. Natl. Acad. Sci. U.S.A.* **2007**, *104*, 20332–7.

(37) Sanchez, J. F.; Lescar, J.; Chazalet, V.; Audfray, A.; Gagnon, J.; Alvarez, R.; Breton, C.; Imberty, A.; Mitchell, E. P. *J. Biol. Chem.* **2006**, *281*, 20171–20180.
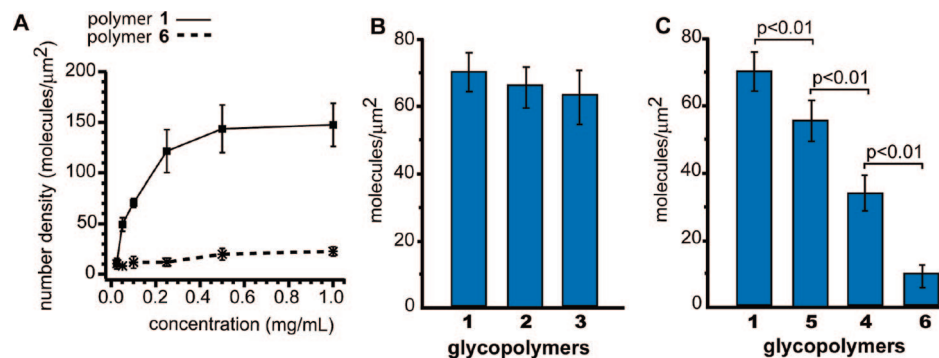
Figure 4. FCS analysis. (A) Surface concentration of mucin mimic polymers as a function of incubation concentration. Solid line: glycopolymer **1** demonstrates concentration dependent incorporation into the cell membrane. Dashed line: glycopolymer **6** does not insert into the cell membranes and exhibits minimal nonspecific binding to the cell surface. (B) Surface densities of mucin mimic polymers with different glycan structures. (C) Surface densities of mucin mimic polymers with different hydrophobic end groups. Error bars represent the standard deviation around the mean values. For all samples p-values were calculated using the Student's t test.

Table 1. Number Density of Glycopolymers (N) in *ldlD* CHO Cell Membranes after Incubation at 100 μg/mL for 1 h, and Their Corresponding Diffusion Coefficients (D) on the Cell Surface

glycopolymer	1	2	3	4	5	6
N (molecules/μm^2)	69 ± 6	66 ± 7	62 ± 8	32 ± 7	54 ± 7	11 ± 5
D (μm^2/s)	0.33 ± 0.04	0.35 ± 0.06	0.29 ± 0.07	0.32 ± 0.06	0.31 ± 0.05	0.05 ± 0.03

known to accumulate in early endosomes.[38] As shown in Figure 6, significant colocalization was observed after a 1 h incubation with polymer **1** at 37 °C.

Further, we explored the dynamics of intracellular trafficking by video microscopy. As shown in Movie 1 (Supporting Information), once internalized into vesicles in *ldlD* CHO cells, the fluorescent polymers appear to move in a directional manner, consistent with trafficking of vesicles along microtubules.[39] As confirmation, we treated the cells with the microtubule disrupting agent nocodazole and the observed internal motion of the glycopolymers ceased (Movie 2, Supporting Information). In summary, the observed localization of polymer **1** in endocytic vesicles and the trafficking properties of the internalized polymer are similar to those of endogenous cell-surface molecules.[32]

Conclusions

In summary, we demonstrated that synthetic glycopolymers can be displayed on live cells by passive insertion into the plasma membrane. Once in the cell-surface environment, these synthetic polymers exhibit behaviors similar to native mucins, such as specific protein binding and internalization through endocytic pathways. A key feature of this study was the application of FCS to simultaneously quantify polymer density and mobility. This technique provided an unprecedented level of molecular characterization in a synthetically engineered cell-based system.

We found polymer insertion efficiency and mobility to be independent of glycan structure. Thus, one should be able to separate the functional consequences of changing the displayed glycan structures from those produced by changes in density or dynamics. The density of the glycopolymers can be controlled independently by varying the solution concentration used for cell surface loading. Furthermore, the hydrophobic end group can be tailored to modulate membrane insertion efficiency and cell surface density. Using this platform, variations in glycan

structure, density, and dynamics can be related to function at the cellular level.

Experimental Methods

General Methods. All chemical reagents were of analytical grade, obtained from commercial suppliers, and used without further purification unless otherwise noted. The fluorescein-conjugated lectin *Helix pomatia* agglutinin (HPA) was purchased from EY Laboratories (San Mateo, CA). All reaction solvents were distilled under a nitrogen atmosphere prior to use. CH_2Cl_2, pyridine, and toluene were dried over CaH_2. Unless otherwise specified, all solvents were removed under reduced pressure using a rotary evaporator. ^{1}H NMR and ^{13}C NMR spectra were obtained at 400 and 100 MHz, respectively, using a Bruker spectrometer. Chemical shifts are reported in parts per million (ppm) relative to tetramethylsilane, and coupling constants (J) are reported in hertz (Hz). Infrared (IR) spectra were obtained using a Perkin-Elmer 1600 Series Fourier transform infrared spectrometer (FTIR). Low- and high-resolution fast atom bombardment (FAB) mass spectra were obtained at the UC Berkeley Mass Spectrometry Laboratory. Electrospray ionization (ESI) mass spectra were obtained with a Hewlett-Packard Series 1100 spectrometer. Gel permeation chromatography (GPC) with THF as an eluent was carried out using a system composed of a Waters 510 pump with a Waters 717 autosampler, 500 Å PLgel columns thermostatted at 35 °C, and an Optilab DSP differential refractometer thermostatted at 35 °C. The GPC data were analyzed using Empower software (Waters) based on polystyrene and polysaccharide standards to calculate the polydispersity (PDI).

Incubation of *ldlD* CHO Cells with Glycopolymers (1−6) for FCS and Fluorescence Microscopy. *ldlD* CHO cells were seeded at a density of 50 000 cells/mL into an 8-well microscopy tray and allowed to grow for 48 h at 37 °C and 5% CO$_2$ in Ham's F-12 medium supplemented with 10% FBS. The cells were rinsed with Ham's F-12 serum-free media (2 × 400 μL), and the media was replaced with 400 μL of Ham's F-12 serum-free media. Polymer **1**, **2**, **3**, **4**, **5** or **6** was added to the cells to afford the desired final concentration of polymer. The cells were then incubated in the presence of polymer for 1 h, Hoechst 33342 dye (1 μg/mL, Invitrogen, Carlsbad) was added for 1 min, the cells were rinsed with serum-free media (3 × 400 μL), and 400 μL of serum-free media were added.

(38) Shurety, W.; Stewart, N. L.; Stow, J. L. *Mol. Biol. Cell* **1998**, *9*, 957–75.
(39) Caviston, J. P.; Holzbaur, E. L. *Trends Cell. Biol.* **2006**, *16*, 530–7.
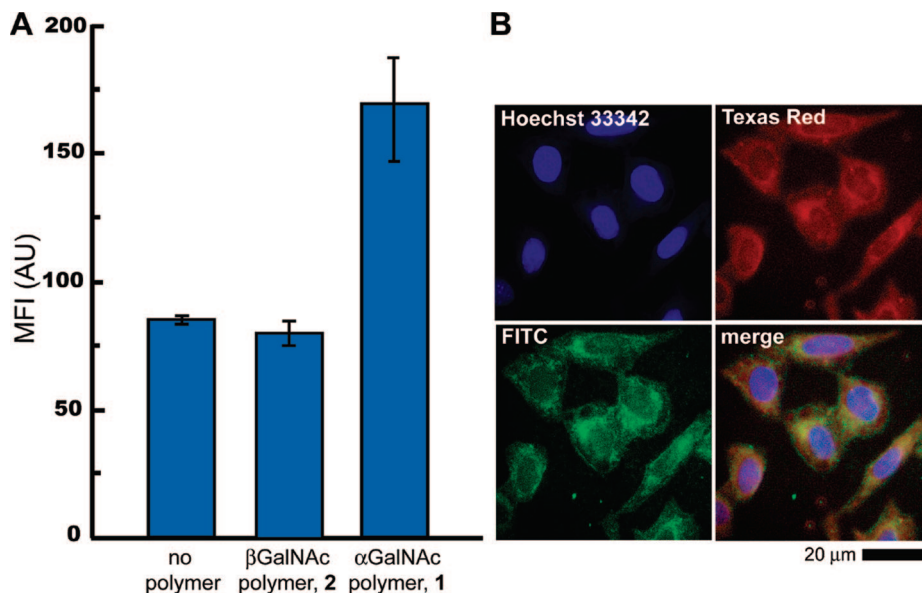
Figure 5. Lectin binding to **1** or **2** displayed on the surface of live *ldlD* CHO cells. (A) *ldlD* CHO cells were incubated with glycopolymers **1** or **2** and then labeled with FITC HPA and analyzed by flow cytometry. MFI = mean fluorescence intensity in arbitrary units (AU). Error bars indicate the standard deviation for three replicate experiments. (B) Fluorescent microscopy images of *ldlD* CHO cells loaded with glycopolymer **1** and stained with FITC HPA. The cells nuclei were stained with Hoechst 33342 before imaging (Blue = DAPI channel, Green = FITC channel, Red = Texas Red channel).
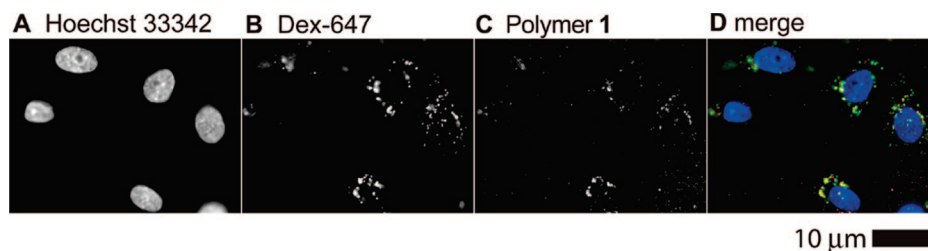

Figure 6. Glycopolymer **1** traffics to early endosomes. (A) Nuclear counterstaining was achieved using Hoechst 33342. (B) Endosome counterstaining was achieved using Alexa Fluor 647 conjugated dextran (Dex-647), a marker for early endosomes. (C) Internalized glycopolymer **1**. (D) Glycopolymer **1** overlaid with Dex-647 and Hoechst 33342.

Fluorescence Cross-Correlation Spectroscopy (FCS). FCS was employed to measure the lateral motilities and to assess the average surface densities of the mucin mimics at the cell plasma membrane. The experiments were performed on an FCS apparatus, constructed in-house, based on a Nikon TE2000 inverted fluorescence microscope that is described in detail by Forstner et al.[40] In brief, a 568 nm beam from a Krypton/Argon mixed gas laser was coupled into the light path of the microscope and focused by the objective (100× magnification, 1.45NA, Nikon Corp., Tokyo, Japan) onto the sample. As individual fluorescently labeled mucin mimics diffuse into this excitation spot, they emit photons that are collected by the objective. After passing through the dichroic mirror, the emission light is first spectrally filtered with a 568 nm notch filter (Kaiser Optical Systems, Ann Arbor, MI) and then spatially filtered by a confocal pinhole aperture (50 μm diameter, Thorlabs, Newton, NJ). A 50/50 beam-splitter divides the incoming light, which is finally focused into two avalanche photo diodes (APD) (Perkin& Elmer, Canada). A hardware correlator (correlator.com, Bridgewater, NJ) translates the photon arrival pulses into intensity fluctuations and calculates the cross-correlation between the two APD signals in real time. The correlation curves are aquired and fitted to analytical expressions in IGOR Pro (WaveMetrics, Lake Oswego, OR) using a nonlinear Levenberg–Marquardt algorithm.

For each condition and compound, we performed correlation measurements on at least five individual cells. For each cell, a

minimum of 10 separate correlation measurements of a 30 s duration were taken and mean values and corresponding standard deviations for every point of the experimental curves were calculated. As it was impossible to rid the solution from all free fluorescently labeled polymers, the correlation curves on cells exhibit two distinct decays. Thus, we fit an analytical form of the temporal cross-correlation $G(\tau)$ that assumes free diffusion of two components with dissimilar diffusion coefficients, of the form:[41]

$$G(\tau) = \frac{1}{N}\left[\left(A\frac{1}{1 + \tau/\tau_{DA}}\right) + \left(B\frac{1}{1 + \tau/\tau_{DB}}\right)\right] \quad (1)$$

Besides the average amount of fluorophores in the excitation area (N) and the two diffusion correlation times (τ_{DA} and τ_{DB}), equation 1 also takes into account the fractions A and B of the total number (N) that exhibit the respective decorrelation times. Using the reciprocal standard deviations as weights, we fitted the average correlation curve for each experiment to equation 1 to extract the correlation times (τ_{DA} and τ_{DB}) associated with the diffusion processes. These times are equivalent to the time it takes for the mean square displacement of a diffusing molecule to reach the size of the effective observation area, ϖ, of the FCS apparatus. Consequently, we evaluated $D_A = \varpi/4\tau_{DA}$ to obtain the diffusion coefficient D_A from the measured time τ_{DA}. The observation area, ϖ, was determined independently using 20 nM Alexa 594 (Invit-

(40) Forstner, M. B.; Yee, C. K.; Parikh, A. N.; Groves, J. T. *J. Am. Chem. Soc.* **2006**, *128*, 15221–15227.

(41) Burns, A. R.; Frankel, D. J.; Buranda, T. *Biophys. J.* **2005**, *89*, 1081–1093.

rogen Corp., Carlsbad, CA) in 50 mM TRIS, pH 10, employing the fluorophore's known diffusion coefficient (341 $\mu m^2/s$) as a standard.[42] Using the resulting effective observation area (ϖ), the total average number density (N), and the fraction (A), we calculated the number N_A of molecules per μm^2 undergoing slow membrane diffusion using $N_A = A * N * (1/\varpi)$. For each experimental condition the diffusion constants and specific number densities determined in individual experiments were averaged. The errors on the experimental values were estimated by the respective standard deviations.

Analysis of Polymer Incorporation into *ldlD* CHO Cell Membranes by Flow Cytometry. *ldlD* CHO cells were seeded at a density of 50 000 cells/mL into a 6-well tissue culture plate and allowed to grow for 48 h at 37 °C and 5% CO_2 in Ham's F-12 medium supplemented with 10% FBS. Solutions of **1** or **2** (1 mg/ mL stock solutions in serum-free media) were added to the individual wells to give the desired final glycopolymer concentration (100 $\mu g/mL$) in a total volume of 2 mL. The cells were incubated with the glycopolymers for 1 h at rt. The cells were lifted from the plate with 1 mM EDTA, pelleted (3000 rpm, 3 min), and transferred to a 96-well V-bottom tissue culture plate. The cells were pelleted, washed with serum-free media and resuspended, and then incubated with FITC-labeled lectin (30 $\mu g/mL$) for 1 h at 4 °C. The cells were washed with serum-free media to remove unbound protein, pelleted, resuspended in serum-free media, and subjected to flow cytometry analysis on an FACSCalibur instrument (BD Biosciences, Franklin Lakes, NJ) equipped with a 488 nm argon laser. All data points were collected in triplicate and reported as the mean fluorescence intensity (MFI) of a population of cells from replicate experiments.

Internalization of 1 and Alexa Fluor 647-Labeled Dextran. *ldlD* CHO cells were seeded into 8-well coverglass tissue culture slides at 30 000 cells/mL and incubated for 48 h at 37 °C. The cells were then rinsed with serum-free media (2 × 400 μL), and the media was replaced with 400 μL of Ham's F-12 medium supplemented with 10% FBS. These cells were incubated with **1** (100 $\mu g/mL$) at 37 °C for 1 h, followed by Hoechst 33342 dye (1 $\mu g/mL$), and with dextran-Alexa Fluor 647 (1 mg/mL) for 5 min at 37 °C and 5% CO_2 in Ham's F-12 medium supplemented with 10% FBS. The cells were then rinsed with serum-free media and

subjected to fluorescence microscopy at 25 °C. Fluorescence images were acquired on a Zeiss Axiovert 200 M inverted microscope (Carl Zeiss MicoImaging Inc., Thornwood NY) equipped with a 63× 1.4 NA PlanApochromat oil immersion lens. Image stacks containing 20 sections, spaced 0.1 μm apart, were acquired using a CoolSNAP HQ CCD camera (Photometrics, Tucson, AZ). The image stacks were digitally deconvolved using the nearest neighbor algorithm of Slidebook (Intelligent Imaging Innovations Inc., Santa Monica, CA).

Intracellular Trafficking Dynamics of Polymer 1. *ldlD* CHO cells were seeded into 8-well coverglass tissue culture slides at 30 000 cells/mL and incubated for 48 h at 37 °C. The cells were then rinsed with serum-free media (2 × 400 μL), and the media was replaced with 400 μL of Ham's F-12 medium supplemented with 10% FBS. These cells were incubated with **1** (100 $\mu g/mL$) at 37 °C for 1 h, followed by Hoechst 33342 dye (1 $\mu g/mL$). A time-lapse movie was acquired using epi-fluorescence with a 100× objective (1.45NA, Nikon Corp., Tokyo, Japan) on a Nikon TE 2000 microscope equipped with a Cascade 512B camera (Princeton Instruments Inc., NJ). Individual images were acquired with a 100 ms exposure every 5 s. The cells were then treated with nocodazole (100 ng/mL) for 1 h and rinsed with serum-free media (2 × 400 μL), and another time lapse movie was acquired using settings noted above.

Supporting Information Available: Synthetic procedures for compounds **4** and **6**; IR, ^{1}H NMR, and GPC data for compounds **4** and **6**; time-lapse movies of polymer motion in cells before and after treatment with nocodazole. This information is available free of charge via the Internet at http://pubs.acs.org/.

JA710644G

(42) Holden, M. A.; Kumar, S.; Castellana, E. T.; Beskok, A.; Cremer, P. S. *Sens. Actuators, B* **2003**, *92*, 199–207.